Senetakis, K. *et al.* (2013) ***Géotechnique Letters*** **3**, No. 2, 59–66, http://dx.doi.org/10.1680/geolett.13.00019

Tangential load–deflection behaviour at the contacts of soil particles

K. SENETAKIS*, M. R. COOP* and M. C. TODISCO*

This paper describes a laboratory investigation of the response of coarse-grained soil particles at their contacts. The tests were carried out in a newly developed micromechanical inter-particle loading apparatus capable of imposing and measuring loads and deflections at the contacts of non-conforming (i.e. non flat-to-flat) surfaces. The apparatus was designed to investigate the behaviour at contacts over a range of load levels from the initial contact stiffness to failure under sliding. The paper presents tests on a variety of particle contacts, investigating the effects of test conditions as well as particle properties and quantifying the particle roughness using an interferometer microscope. The initial tangential load–deflection behaviour is shown to be highly non-linear and predominantly plastic. The stiffness depends on the normal load applied and the particle type, but does not degrade with small numbers of cycles. Shearing led to a significant decrease in the amplitude of the surface roughness of the particles, mostly through the removal of asperities, which shows that the tangential stiffness might not be significantly affected by the amplitude of surface roughness.

KEYWORDS: discrete-element modelling; friction; laboratory tests; particle-scale behaviour; sands; stiffness

NOTATION

F_N	normal load
F_T	tangential load
$F_{T,max}$	maximum tangential load
K_T	tangential stiffness
K_{T0}	initial tangential stiffness
S_q	surface roughness corresponding to the root mean square deviation of the heights of the surface
δ	horizontal displacement
δ_{ref}	horizontal displacement at the onset of the steady-state sliding
μ_{dyn}	coefficient of dynamic friction
μ_{st}	coefficient of static friction

INTRODUCTION

Previous experimental studies of the response at the contacts of naturally occurring particles have often focused on the normal load–deflection response and the corresponding normal stiffness (e.g. Cole & Peters, 2007, 2008; Cole *et al.*, 2010) or the frictional characteristics with respect to inter-particle shearing tests (e.g. Horn & Deere, 1962; Skinner, 1969; Cole *et al.*, 2010; Cavarretta *et al.*, 2011). Even if it is potentially an important input in simulations that utilise the discrete element method (DEM) (Cundall & Strack, 1979), the tangential force–displacement response and the corresponding tangential stiffness, in particular for the case of contacts between minerals such as quartz, have received less attention in experimental research.

There are numerous contact models available for DEM, especially for particle flow applications, but in soil mechanics the range used tends to be limited. One of the simplest models is a linear spring–dashpot (Walton, 1983), which may be adopted for both the normal and tangential directions, often linking the two spring stiffnesses but assuming fixed values, so that the tangential stiffness remains constant no matter what the normal force, F_N. A frictional limit to the tangential force is generally introduced at $F_T = \mu F_N$, where F_T is the tangential force and μ the coefficient of inter-particle friction. Thornton *et al.* (2011) showed that, for analysis of particle impacts, this simple type of model can be just as accurate as more complex models, with the advantage that it is computationally much more efficient.

Many of the more complex models are based on a combination of the models of Hertz (1882) for normal loading and Mindlin & Deresiewicz (1953) (M&D) for tangential loading. This is derived from the contact of two elastic spheres although, in the tangential direction, hysteretic and plastic displacements are allowed (arising from 'micro-slips' at the contact) so that there is a gradual decay of the tangential stiffness from an initial elastic value that depends on the geometry and elastic properties of the spheres to zero as $F_T = \mu F_N$ is approached. To achieve this decay, the initial stiffness is multiplied by $(1 - F_T/\mu F_N)^{1/3}$ for a monotonic increase of F_T at constant F_N. On load reversal, the initial elastic stiffness is unchanged but the rate of decay is reduced to achieve the hysteresis loop. The initial tangential stiffness depends on the contact area and so is proportional to $F_N^{2/3}$.

There are several simplified versions of the Hertz–M&D models (e.g. Langston *et al.*, 1995; Di Renzo & Di Maio, 2004). Walton & Braun (1986) proposed a simplified tangential model in which a stiffness decay similar to the M&D model is assumed. This can be combined either with Hertzian normal contact behaviour or with the simplified model of Walton (1993) in which the normal load–deflection behaviour is linear but a higher stiffness is assumed in unloading, giving residual displacements. Here the tangential stiffness is assumed proportional to the normal stiffness and so is independent of F_N. This was later modified by Vu-Quoc & Zhang (1999) to allow better modelling of combined changes of F_T and F_N. Vu-Quoc *et al.* (2004) introduced plasticity into their contact model, based on finite-element analyses of elasto-plastic spheres. They found that if the normal load was beyond yield then

Manuscript received 22 February 2013; first decision 20 April 2013; accepted 15 May 2013.
*Department of Civil and Architectural Engineering, City University of Hong Kong, Kowloon Tong, Hong Kong

the tangential stiffness was increased, largely as a result of the increased contact area compared to the Hertz model. However, under combinations of normal and tangential load, decreased tangential stiffness could be observed as a result of the decrease in tangential stiffness due to the plastic strains. In a modelling study of ultrafine limestone powders, Tomas (2007) assumed smooth surfaces but with a soft contact compared to stiff particles, so that yield occurred at very small contact displacements. The normal load–displacement behaviour was therefore much softer than Hertz, with a consequent effect on the tangential stiffness through the increased contact area. The adhesion that Tomas allowed for ultrafine particles would be insignificant for the large particles tested here, but in any case Cavarretta *et al.* (2010) showed that the normal load–displacement behaviour of sand-sized particles was basically Hertzian, although with some possible initial plasticity arising from asperity yielding, which was not modelled by Tomas (2007).

With respect to laboratory investigations, Cole *et al.* (2010) provided some extremely useful data for the tangential load–deflection response at the contacts of naturally occurring materials, but their study focused on a flat–sphere type of contact with limited information for a sphere–sphere type, which is the ideal case for real soils. Their tests were also mostly on prepared surfaces for the contact of a perfect sphere and a flat surface of gneiss rather than on inter-particle tests on natural sand grains of a single mineral. The large size of the sphere (about 15 mm diameter) together with the mixed mineralogy of the rock meant that the behaviour they observed might be more applicable to the overall rock than individual minerals since the contact point between the sphere and the flat might comprise more than one mineral. Overall, Cole *et al.* (2010) observed that the response at the contacts of minerals is highly hysteretic and plastic with a reduction of the surface roughness on the shearing track, but the latter was observed on flat-type surfaces.

This paper presents the main findings from a series of inter-particle shearing tests at the contacts of soil particles of a single mineral and of a particle–particle type with focus on the tangential force–displacement and stiffness degradation–displacement in the range of very small deformations. Monotonic and cyclic shearing tests were performed at the contacts of dry and saturated soil particles of variable types about 1–5 mm in size. A new technique was also adopted in order to investigate the effect of shearing on the surface characteristics of particles, which might provide better understanding of the nature of frictional response.

EQUIPMENT, MATERIALS AND PROCEDURES

The inter-particle shearing tests were performed in a newly developed micro-mechanical loading apparatus (Figs 1 and 2). The device is computer-controlled and is capable of imposing and measuring forces and deflections in the normal and tangential directions at the contacts of soil particles of particle–particle type (which is of major interest in soil mechanics) in the range of very small displacements of less than 1 μm up to about 400 μm. Of key importance during the design and development of the apparatus was the performance of shearing tests at very small normal forces, of the order of 0·5–5 N, which represent more realistically the normal forces developed at the contacts of soil particles for common engineering isotropic pressures (Barreto, 2009).

Strong quartz particles of Leighton Buzzard sand (LBS) and weak particles of a crushed limestone (LMS) of size 1·18–5·00 mm were tested in both monotonic and cyclic inter-particle shearing tests of a force-controlled type at loading rates of 1·5–10 N/h. The tests were all conducted with apex-to-apex contacts to avoid inclined loading. This condition was ensured by aligning the particles using two orthogonally placed microscopes orientated along the direction of shear and perpendicular to it. A check on the apex contact could be made when the initial normal load was applied – if a significant shear force was measured on contact, then that was taken as an indication that the contact was not horizontal.

In order to study the possible mechanisms that control the frictional characteristics and tangential stiffness development at the contacts of the particles, the amplitude of the surface roughness of the particles was generally evaluated before the shearing tests and also after the completion of the experiments in some cases. For this purpose, white light interferometry (Altuhafi & Coop, 2011) was used, flattening the surfaces in the software of the interferometer in order to avoid the possible influence of curvature of the particle shape. The LBS particles showed a surface roughness with an average value of 0·38 μm and a standard deviation of $\pm 0{\cdot}19$ μm; the LMS particles were rougher, with an average value of 1·01 μm with standard

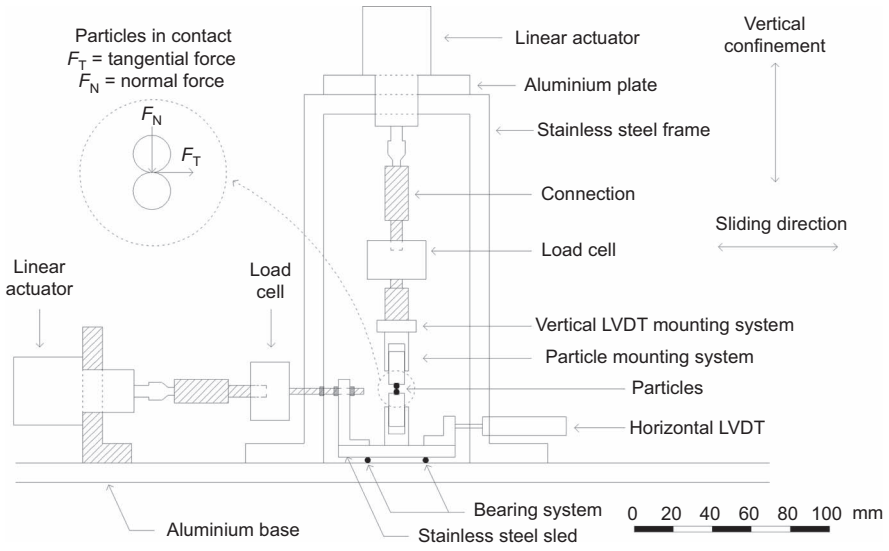

Fig. 1. General scheme of the inter-particle loading apparatus

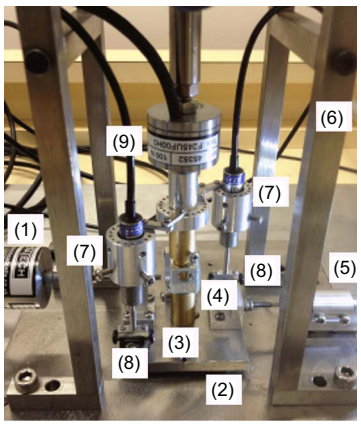

Fig. 2. Close-up view of the apparatus: (1) load cell for horizontal force; (2) stainless steel sled; (3) particle mounting system; (4) cell for immersing particles in water; (5) linear variable differential transformer (LVDT) for horizontal deflection; (6) stainless steel frame for mounting the vertical system; (7) LVDTs for vertical deflection; (8) linear bearing for mounting LVDTs on the sled; (9) load cell for vertical load

deviation of $\pm 0{\cdot}19$ μm. These values were calculated by the root mean square (RMS) deviation of the heights of the surface (S_q) (Altuhafi & Coop, 2011) using a measuring area of 20 μm × 20 μm in the interferometer in order to achieve sufficient resolution. Figure 3 shows a typical three-dimensional view of the surface of a particle of the crushed limestone (the image has been flattened to remove particle curvature).

RESULTS

Typical load–deflection responses and stiffness degradation for quartz particles

Typical tangential force–displacement and stiffness degradation–displacement diagrams for the contacts of dry and saturated quartz particles are presented in Figs 4–6. Before the onset of sliding, in general at between 0·1 and 0·4 μm in most experiments, the tangential force increased rapidly. Beyond a displacement of about 2 to 5 μm, a steady state was observed with continued shearing taking place under a constant shear force. For the small range of horizontal displacements used in the tests presented here there was no significant vertical displacement and so no need to correct for the rotation of the stresses as was done by Cavarretta *et al.* (2011) for tests over larger displacements. This is confirmed by the constant ratio of F_T/F_N that was reached in all tests. The coefficient of static friction μ_{st}, defined as the ratio between the maximum tangential force $F_{T,max}$ and F_N, was not significantly affected by the conditions of the test (i.e. dry or saturated surfaces), but the data were a little scattered with values in the range 0·12–0·35 for the quartz particles. The coefficient of dynamic friction μ_{dyn}, which corresponds to steady-state sliding, was equal to or very slightly lower than μ_{st}.

There was a general trend of increasing initial stiffness K_{T0} with increasing normal load, but the different pairs of particles showed some scatter in the K_{T0} values. Assuming linearity, the K_{T0} values ranged between about 0·05 and 0·70 N/μm, depending primarily on the normal load and the displacement at which the initial stiffness was evaluated.

At first sight, the overall increase of the tangential force seems to be approximately linear at small deformations and the F_T–δ diagrams may be expressed with the bi-linear model of Fig. 7 commonly adopted in DEM simulations. However, a detailed evaluation of the force–displacement curves by calculating tangent stiffnesses reveals non-linear behaviour throughout. This is in qualitative agreement with the experimental findings of Cole *et al.* (2010). The non-linearity in the tangential force–displacement relationship at extremely small shear deformations has been also described mathematically by Johnson (1985) for the case of elastic smooth spheres in contact. The general shape of the stiffness decay is similar to that expected from the M&D model, although numerical comparisons are difficult because the data are not accurate enough to define the initial stiffness. The effect of the normal load on the stiffness is clear in Figs 4 and 6, even if there is some data scatter in Fig. 6. The effect of the normal load on the

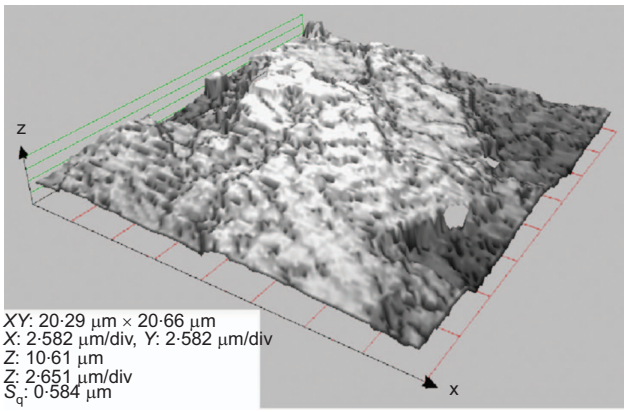

Fig. 3. Typical flattened three-dimensional view of the surface of a particle of crushed limestone through white light interferometry (note that the selected area *XY* is 20·29 μm × 20·66 μm and the scale of the vertical axis is 2·651 μm/div)

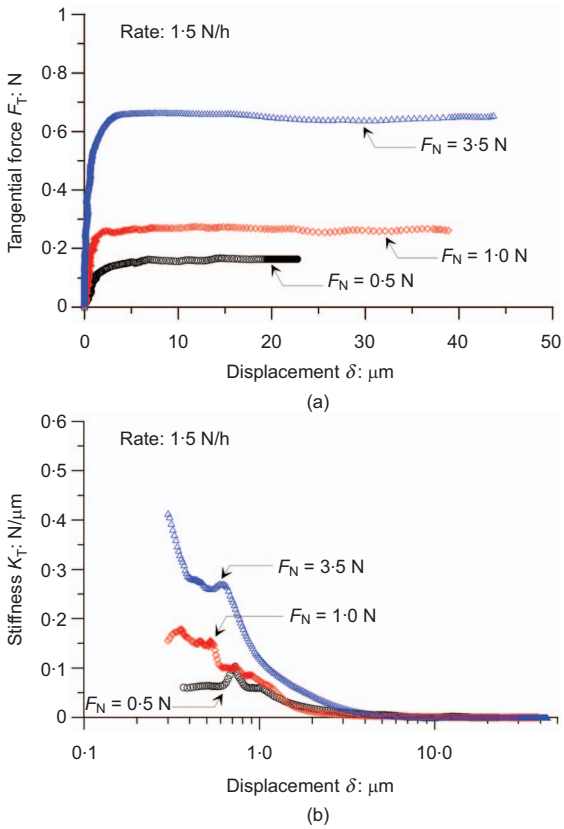

Fig. 4. Effect of normal load on (a) tangential force and (b) stiffness degradation with increasing displacement at the contacts of dry quartz particles

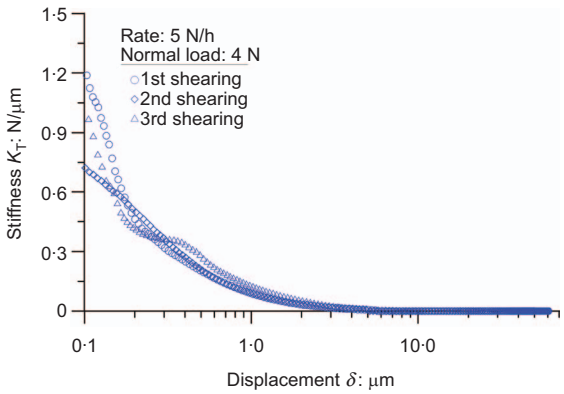

Fig. 5. Effect of loading history on the stiffness degradation–displacement relationship at the contacts of dry quartz particles at a normal load of 4 N

stiffness appears to be of similar magnitude to that predicted by the Hertz–M&D model (i.e. proportional to $F_N^{2/3}$), but more data are needed to confirm this. A comparison of Figs 4–6 also reveals that, within the data scatter, there is no noticeable effect of whether the particles were wet or dry, although it should be noted that the 'dry' tests were carried out in a laboratory in which the ambient humidity is typically around 93–97%. Repeated loading at the same contact point (Fig. 5) had no effect on the stiffness degradation.

Effect of soil particle type

Representative monotonic shearing tests on particles of crushed limestone are presented in Fig. 8. Comparison of this figure with Figs 4–6 reveals that μ_{st} and μ_{dyn} are lower for the weak particles of limestone than the quartz particles, with values ranging between 0·07 and 0·09. In addition, the type of particles had an important effect on the tangential stiffness, with the limestone particles having K_T values approximately two to four times lower than those of the quartz particles at a displacement of 0·5 μm. Even if the limestone particles had values of surface roughness about two to four times higher than the quartz, their coefficients of friction and the initial tangent stiffnesses were significantly lower. Within the M&D model, the initial tangential stiffness should be dependent on the elastic properties of the materials, but the Young's modulus of quartz is 94–98 GPa and that of calcite is 73–84 GPa, while the shear moduli are 44–46 GPa and 28–32 GPa, respectively (Mavko *et al.*, 1998; Jaeger *et al.*, 2007).

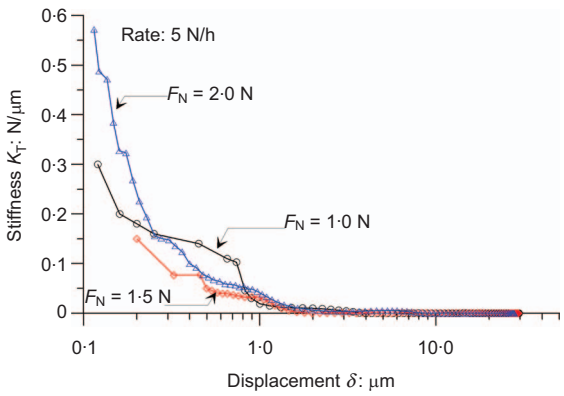

Fig. 6. Effect of normal load on stiffness degradation at the contacts of saturated quartz particles

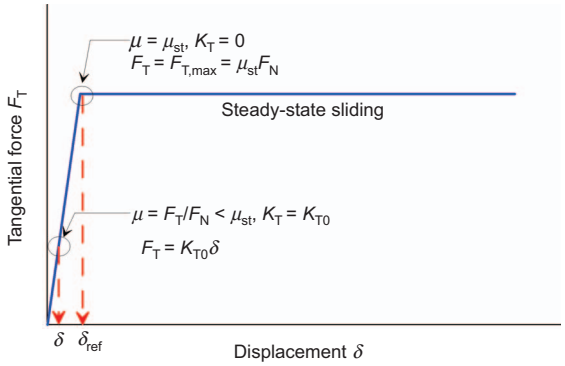

Fig. 7. Common bi-linear tangential force–displacement law (μ = coefficient of friction, μ_{st} = coefficient of static friction at the onset of maximum tangential force, K_T = tangential stiffness, K_{T0} = initial tangential stiffness before the steady-state sliding, δ_{ref} = displacement at the onset of the steady-state sliding, F_N = normal load)

This therefore does not seem to be able to explain the very different tangential stiffnesses measured. The key differences in the properties of the quartz sand and limestone particles that may explain the different stiffnesses and values of μ are then in their hardnesses (7 and 3, respectively, on the Mohs scale) and in the particle strengths; single-particle crushing tests gave mean strengths of 50 MPa for the quartz and 13 MPa for the limestone. The asperity strength may be related to the particle strength, and this may influence the tangential loading behaviour.

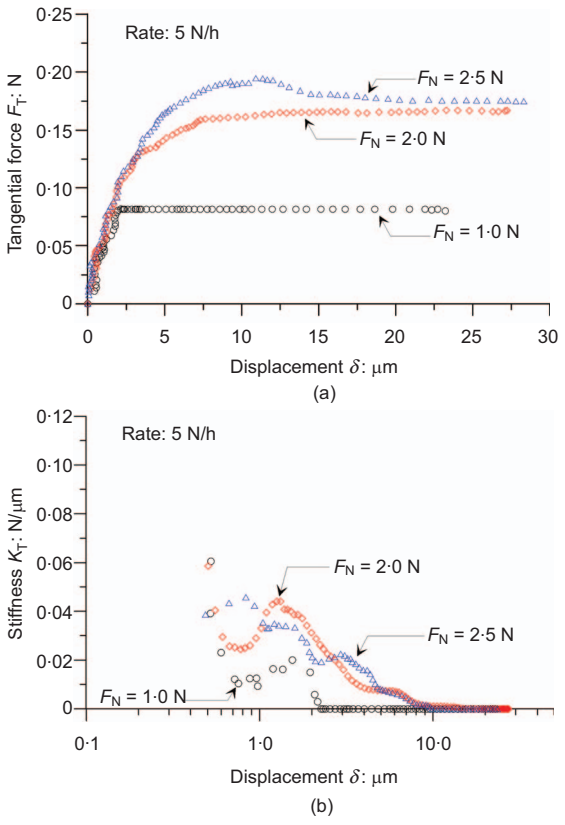

Fig. 8. Effect of normal load on (a) tangential force and (b) stiffness degradation with increasing displacement at the contacts of dry particles of crushed limestone

Unload–reload behaviour

A series of unload–reload cycles showed that the displacements before the onset of sliding at the constant steady state are largely plastic. Typical cyclic tests on dry quartz particles are shown in Fig. 9 and on dry particles of crushed limestone in Fig. 10. In Fig. 9, the results from a monotonic loading test at the same strain rate and normal load that was executed on the same pair of particles indicated good agreement between the monotonic and cyclic load–deflection curves.

Cole *et al.* (2010) showed that, before the onset of a steady-state sliding, the response at the contacts of the gneiss they tested was hysteretic. The results of Figs 9 and 10 show that the behaviour for unload–reload loops prior to and after full mobilisation of μ_{dyn} is similar. The data are not sufficiently accurate to be able to resolve the stiffness in unload–reload, and some inaccuracy in the data even gives an increase in displacement during unloading in a few cases. But it seems that for the quartz the behaviour is largely elastic, the unloading and reloading data coinciding, with a very much higher overall stiffness than for first loading. Although the data are not accurate enough to make detailed comparisons, the decay in stiffness during unloading seems less rapid than might be expected from the M&D model, giving a larger residual displacement. For the limestone particles, the divergence of the reloading data from the unloading curve occurs much earlier than for the quartz. These data suggest that for particle–particle type contacts, the main mechanism of friction may be due to inter-locking and breakage of the asperities on the nano- to micro-scale level. This mechanism should be further examined since it is possibly an important factor for energy dissipation in particulate media even at extremely small strains. The data from this study, as well as the results of Cole *et al.* (2010), show that the theoretical tangential force–displacement models adopted in DEM simulations should also consider this overall much higher tangential stiffness during unload–reload loops in comparison to the initial loading.

Evaluation of the sheared surfaces using white light interferometry

The effect of shearing on the surfaces of quartz particles and possible damage to the asperities was evaluated on a representative pair of quartz particles by measuring the surface roughness in the vicinity of the contact area before and after the performance of an inter-particle shearing test. The particles were placed on mounts as shown in Fig. 11.

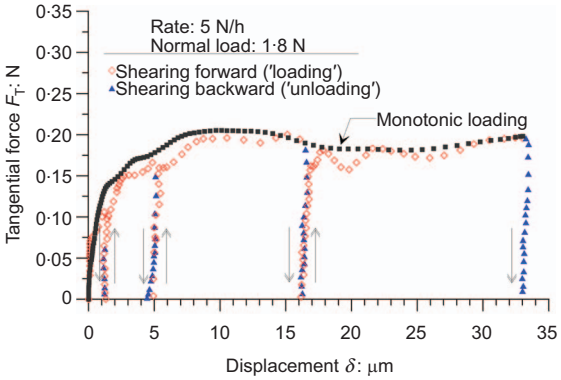

Fig. 9. Response for contacts of dry quartz particles during a series of shearing unloading and reloading cycles at a normal load of 1·8 N and the corresponding response under monotonic loading

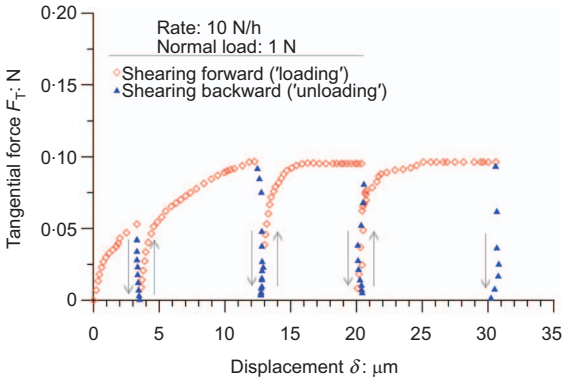

Fig. 10. Response for contacts of dry particles of crushed limestone during a series of shearing unloading and reloading cycles at a normal load of 1 N

Two markers were positioned diametrically opposite each other as reference points to ensure that exactly the same image area was examined before and after the test and that the direction of shearing in the apparatus was known to correspond exactly with the y-direction, passing through the apex of the particle. The mounts were placed on the base of the interferometer and the edges of the markers were located in the interferometer image to ensure correct positioning. The topography of the particles was initially obtained as a two-dimensional image and a comparison of the surface roughness before and after the shearing test could be conducted. In order to ensure that the detected area after the test matched that before with a satisfactory accuracy, the locations of some visible landmarks (i.e. the dips highlighted by rectangular markers in Fig. 12) were examined. From this check it was estimated that the accuracy of the positioning on the apex of the particle was about $\pm 0{\cdot}005$ mm.

Based on the visible landmarks of Fig. 12 (D1, D2, A1, A2, A3), horizontal sections were made at those sections to compare the surface roughness values. Representative sections before and after the test are shown in Fig. 13, with the corresponding amplitude roughness values (RMS) shown in Table 1. There is a marked decrease in the roughness after shearing and evidence that indicates that the asperities on the particles are removed during shearing, making the surface of the particle smoother. It appears from the images that the asperities have been broken off rather than undergone a

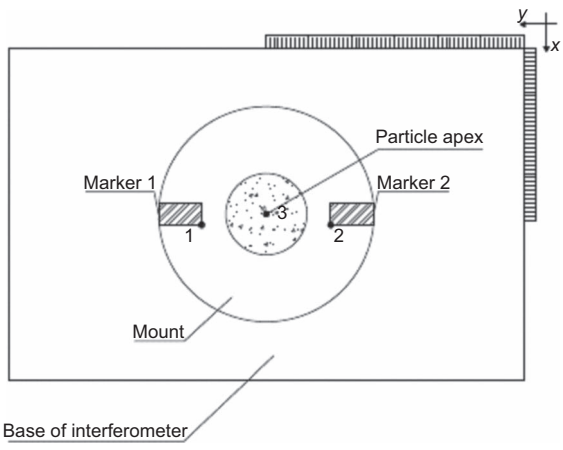

Fig. 11. Positioning of the particle on the base of the interferometer in order to evaluate surface roughness before and after the shearing test

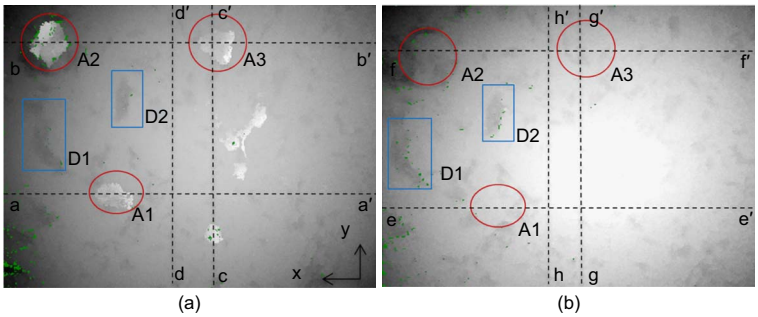

Fig. 12. Surface of particle (a) before and (b) after the shearing test (image size 141·5 μm × 106·8 μm)

plastic deformation. Note that the surface roughness values presented in Table 1 were evaluated using a measuring area of about 140 μm × 140 μm in the interferometer. For sand grains that undergo many cycles of loading through their geological and engineering loading history, making many inter-particle contacts, this type of local decrease in

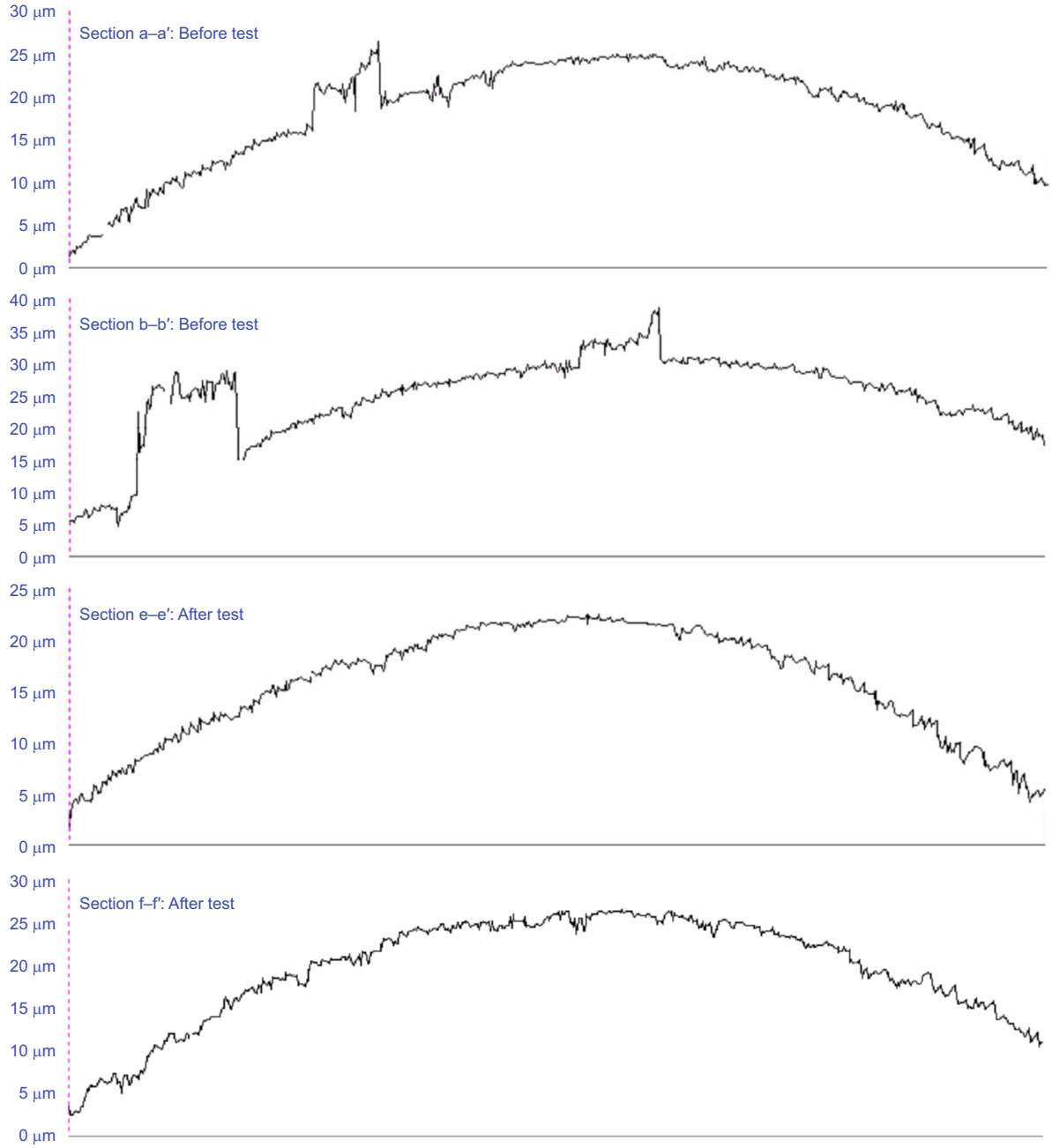

Fig. 13. Interferometer sections of quartz particle before and after the shearing test (note that the horizontal size is 141·5 μm for sections a–a', b–b', e–e' and f–f')

Table 1. Surface roughness values of quartz particle before and after the test

Before test		After test		Reduction
Section	RMS: μm	Section	RMS: μm	in RMS: %
a–a′	1·13	e–e′	0·83	26
b–b′	1·91	f–f′	0·72	62
c–c′	1·23	g–g′	0·83	33
d–d′	0·79	h–h′	0·69	13

roughness might influence a substantial proportion of the particle surface, which may then have a significant effect on the behaviour of newly made contacts.

It is not known to what extent the decrease in roughness is because of the normal force, tangential force or coupled effects. If, as seems likely, the application of a tangential force contributes to asperity breakage, then shearing cycles may reduce the roughness significantly. These cycles did not, however, affect the tangential stiffness (Fig. 5), which may be another indication that roughness does not control tangential stiffness or perhaps that the reduction in roughness was not sufficient to change the stiffness. This mechanism should be further investigated since only a limited number of tests were performed in this study.

CONCLUSIONS

A series of inter-particle monotonic and cyclic shearing tests on pairs of quartz and crushed limestone particles was carried out in a newly developed micro-mechanical apparatus, examining the behaviour at small displacements in particular. The amplitude of the surface roughness of the particles before and after the shearing tests was investigated using white light interferometry and the data indicated that there was a substantial decrease of roughness due to loading.

It was revealed that, before steady-state sliding occurred, the response at the contacts of soil particles was highly non-linear and predominantly plastic. The tangential stiffness was affected by the normal load and the type of soil particles but it was practically unaffected by repeating monotonic loading or, alternatively, by the decrease in the amplitude of the surface roughness. The stronger quartz particles showed a substantially higher initial tangential stiffness in comparison to the weaker particles of crushed limestone, even if the latter had a larger amplitude of mean surface roughness. These data therefore indicate that the amplitude of surface roughness might not be the most important factor in tangential stiffness development. Although the stiffness decay measured in monotonic tangential loading is qualitatively similar to that predicted by contact models for elastic spheres such as the M&D model, such models would not predict the large difference in stiffness between the two particle types and also would not capture the high stiffness in unload–reload cycles. It may be that mineral hardness and/or asperity strength are more influential than elastic stiffnesses.

Overall, the newly developed apparatus was designed to study the response at the contacts of soil particles in both monotonic and cyclic loading in the range of very small normal loads which are of interest for soil mechanics applications. This advanced inter-particle shearing device along with the use of advanced equipment for the determination of the surface roughness characteristics may lead to new directions in the study of the micro-mechanical properties and the mechanisms that dominate the response at the contacts of soil particles. In particular, the ability to control the normal and tangential loads independently while making accurate measurements of the displacements offers the possibility of making significant inroads in the understanding of the effects of combined loads on particle interactions, which is of significant interest to DEM modellers (e.g. Vu-Quoc & Zhang, 1999).

Acknowledgements

The authors are grateful to Dr B. Baudet of the University of Hong Kong for kindly permitting use of the interferometer and to Dr B. N. Madhusudhan of the University of Hong Kong for his help in carrying out the interferometer tests. The technicians from City University of Hong Kong, Mr L. C. Mac and Mr C. K. Lai and the Senior Technical Officer Mr K. H. Chu are acknowledged for their technical support during the development of the new custom-built apparatus. This research work was fully supported by a strategic research grant 7002667 entitled 'The development of a new soil particle loading apparatus' funded by the City University of Hong Kong.

REFERENCES

Altuhafi, F. N. & Coop, M. R. (2011). Changes to particle characteristics associated with the compression of sands. *Géotechnique* **61**, No. 6, 459–471.

Barreto, D. (2009). *Numerical and experimental investigation into the behaviour of granular materials under generalised stress states*. PhD thesis, Imperial College of Science, Technology and Medicine, University of London, UK.

Cavarretta, I., Coop, M. R. & O'Sullivan, C. (2010). The influence of particle characteristics on the behavior of coarse grained soils. *Géotechnique* **60**, No. 6, 413–423.

Cavarretta, I., Rocchi, I. & Coop, M. R. (2011). A new interparticle friction apparatus for granular materials. *Canad. Geotech. J.* **48**, No. 12, 1829–1840.

Cole, D. M. & Peters, J. F. (2007). A physically based approach to granular media mechanics: grain-scale experiments, initial results and implications to numerical modeling. *Gran. Matter* **9**, 309–321.

Cole, D. M. & Peters, J. F. (2008). Grain-scale mechanics of geologic materials and lunar simulants under normal loading. *Gran. Matter* **10**, 171–185.

Cole, D. M., Mathisen, L. U., Hopkinks, M. A. & Knapp, B. R. (2010). Normal and sliding contact experiments on gneiss. *Gran. Matter*, **12**, 69–86.

Cundall, P. A. & Strack, O. D. L. (1979). A discrete numerical model for granular assemblies. *Géotechnique* **29**, No. 1, 49–65.

Di Renzo, A. & Di Maio, F. P. (2004). Comparison of contact-force models for the simulation of collisions in DEM-based granular flow codes. *Chem. Engng Sci.* **59**, No. 3, 525–541.

Hertz, H. (1882). Über die Berührung fester elastischer Körper. *J. Reine Ange. Math.* **92**, 156–171.

Horn, H. M. & Deere, D. U. (1962). Frictional characteristics of minerals. *Géotechnique* **12**, No. 4, 319–335.

Jaeger, J. C., Cook, N. G. W. & Zimmerman, R. (2007). *Fundamentals of rock mechanics,* 4th edn. Oxford: Wiley-Blackwell.

Johnson, K. L. (1985). *Contact mechanics*. Cambridge: Cambridge University Press.

Langston, P. A., Tüzün, U. & Heyes, D. M. (1995). Discrete element simulation of granular flow in 2D and 3D hoppers: dependence of discharge rate and wall stress on particle interactions. *Chem. Engng Sci.* **50**, No. X, 967–987.

Mavko, G., Mukerji, T. & Dvorkin, J. (1998). *The rock physics handbook: tools for seismic analysis in porous media*. Cambridge: Cambridge University Press.

Mindlin, R. D. & Deresiewicz, H. (1953). Elastic spheres in contact under varying oblique forces. *J. Appl. Mech. ASME* **20**, 327–344.

Skinner, A. E. (1969). A note on the influence of interparticle friction on shearing strength of a random assembly of spherical particles. *Géotechnique* **19**, No. 1, 150–157.

Thornton, C., Cummins, S. J. & Cleary, P. W. (2011). An investigation of the comparative behaviour of alternate contact force models during elastic collisions. *Powder Technol.* **210**, No. 3, 189–197.

Tomas, J. (2007). Adhesion of ultrafine particles – a micromechanical approach. *Chem. Engng Sci*. **62**, No. 7, 1997–2010.

Vu-Quoc, L. & Zhang, X. (1999). An accurate and efficient tangential force–displacement model for elastic-frictional contact in particle-flow simulations. *Mech. Mater*. **31**, 235–269.

Vu-Quoc, L., Lesburg, L. & Zhang, X. (2004). An accurate tangential force–displacement model for granular-flow simulations: contacting spheres with plastic deformation, force-driven formulation. *J. Comp. Phys.* **196**, 298–326.

Walton, O. R. (1984). Application of molecular dynamics to macroscopic particles. *Int. J. Engng Sci.* **22**, No. 8–10, 1097–1107.

Walton, O. R. (1993). Numerical simulation of inelastic, frictional particle–particle interactions. In *Particulate two-phase* flow (Roco, M. C. (ed.)). Stoneham, MA: Butterworth-Heinemann, pp. 884–911.

Walton, O. R. & Braun, R. L. (1986). Viscosity, granular-temperature, and stress calculations for shearing assemblies of inelastic, frictional disks. *J. Rheology* **30**, No. 5, 949–980.